Journal of Crystal Growth 310 (2008) 4503–4506

Contents lists available at ScienceDirect

Journal of Crystal Growth

journal homepage: www.elsevier.com/locate/jcrysgro

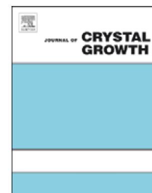

Influence of Zn/O flux ratio and Mn-doped ZnO buffer on the plasma-assisted molecular beam epitaxy of ZnO on *c*-plane sapphire

J.S. Wang [a,*], C.S. Yang [b], M.J. Liou [a], C.X. Wu [a], K.C. Chiu [a], W.C. Chou [c]

[a] Department of Physics and Center for Nano-Technology, Chung Yuan Christian University, Chung-Li 32023, Taiwan
[b] Graduate Program in Electro-optical Engineering, Taipei 10452, Taiwan
[c] Department of Electrophysics, National Chiao Tung University, Hsin-Chu 30010, Taiwan

ARTICLE INFO

Article history:
Received 2 June 2008
Received in revised form
28 July 2008
Accepted 30 July 2008
Communicated by D.P. Norton
Available online 6 August 2008

PACS:
81.15.Hi
81.10.Aj
81.40.Tv
78.55.−m
68.60.−p

Keywords:
A1. Characterization
A1. Reflection high-energy electron diffraction
A3. Molecular beam epitaxy
B1. Oxides
B1. Zinc compounds
B2. Semiconducting II–VI materials

ABSTRACT

This work investigated the influence of Zn/O flux ratio and Mn-doped ZnO buffer layer on the epitaxial growth of ZnO grown by plasma-assisted molecular beam epitaxy on *c*-plane sapphire substrates. Atomic force microscopy (AFM), photoluminescence (PL) and X-ray diffraction (XRD) measurements indicated that a small amount residual strain of ZnO epilayers was further relaxed under stoichiometric growth conditions due to the better surface migration of the adatoms. Moreover, we observed that a small amount of Mn doping led to obtain a flatter surface with stronger lattice relaxation maybe due to the greatly enhanced surface migration of the adatoms. By adding a Mn-doped ZnO buffer layer the optical and electrical properties of the ZnO epilayers had significant improvement.

© 2008 Elsevier B.V. All rights reserved.

1. Introduction

Wurtzite-structure ZnO with a wide direct band gap of 3.37 eV at room temperature (RT) has a large exciton binding energy of 60 meV. The fundamental properties of ZnO make it an attractive candidate for UV light-emitters or laser diodes. Optical pumped excitonic lasing at RT from ZnO has been reported [1,2], and excitonic-stimulated emissions have been observed at temperatures up to 550 °C [3]. Another possible application of ZnO is in the field of spintronics [4,5]. After Dietl et al. [6] predicted RT ferromagnetism for Mn-doped ZnO, a number of studies have been carried out experimentally and theoretically to obtain reliable Mn-doped ZnO diluted magnetic semiconductors [7–9].

Due to the hexagonal symmetry and low cost, ZnO epitaxial layers grown by plasma-assisted molecular beam epitaxy (PA-MBE) have mostly been studied using c-plane sapphire as a substrate [10–13]. However, there is a large in-plane lattice mismatch (18%) and two types of in-plane rotation domains between c-oriented ZnO and the oxygen sublattice of *c*-plane sapphire (ZnO[1 $\bar{1}$ 0 0]||Al_2O_3[1 1 $\bar{2}$ 0] and ZnO[1 1 $\bar{2}$ 0]||Al_2O_3[1 1 $\bar{2}$ 0]). These 30°-rotation domains are surrounded by highly defective domain boundaries with threading dislocations leading to deterioration of the crystal quality [14,15]. Therefore, the lattice strain relaxation and accompanying structural evolution in the initial growth stage directly affect the surface morphology and the crystalline quality [16,17]. Low-temperature ZnO homo-buffer layers have been tried to reduce the defects and dislocation density caused by the large lattice mismatch [18,19]. To eliminate the hexagon-on-hexagon growth (ZnO[1 1 $\bar{2}$ 0]||Al_2O_3[1 1 $\bar{2}$ 0]), some researchers have suggested that depositing a thin MgO hetero-buffer layer, which has lattice mismatch of −8.4% and 9.1% between ZnO and sapphire, respectively, at the interface between ZnO and *c*-plane sapphire [20,21]. Furthermore, a dopant can influence both the kinetic and thermodynamic factors in the

* Corresponding author. Tel.: +886 3 2653210; fax: +886 3 2653299.
E-mail address: jswang@cycu.edu.tw (J.S. Wang).

0022-0248/$ - see front matter © 2008 Elsevier B.V. All rights reserved.
doi:10.1016/j.jcrysgro.2008.07.108

formation and growth of grains during film deposition. Kim et al. [22] demonstrated that Mn doping (Mn = 5%) greatly enhanced the atomic alignment and led to a singly oriented film by totally suppressing the hexagon-on-hexagon growth. Han et al. [23] reported that ZnO doped with Mn increased the surface diffusion. Nakayama et al. [24] showed that a $Zn_{0.95}Mn_{0.05}O$ thin film is preferentially oriented along the [0 0 0 1] axis and that the interface and surface are very flat.

In this work, we present our study on the growth of ZnO epilayers varying with Zn/O flux ratio and the improvements in crystal structures, optical and electrical properties by using a Mn-doped ZnO buffer layer at the interface between ZnO and c-plane sapphire substrates grown by PA-MBE.

2. Experiment

The growth was carried out in a Veeco EPI 620 MBE system. An Addon RF-plasma source with independently separated pumping design was used to provide reactive oxygen radicals. The flux of oxygen gas was controlled by a mass flow controller system. Knudsen-cells were used for evaporating Zn and Mn metal sources. Before deposition, the *c*-plane sapphire substrates were cleaned by acetone and chemical etched by the heated acid solution of H_2SO_4 and H_3PO_4 for 15 min. Following, the substrate was desorbed at 920 °C. During growth, the substrate temperature was fixed at 650 °C and the oxygen RF–plasma source was kept at 300 W with an oxygen flow rate of 1.5 SCCM. The whole growth process was monitored by reflection high-energy electron diffraction (RHEED). Film thickness was measured by employing the cross-sectional scanning electron microscope (SEM). After growth, the samples were investigated by atomic force microscopy (AFM), X-ray diffraction (XRD), Hall measurements, and photoluminescence (PL) spectroscopy. A 325 nm of He–Cd laser was employed as the exciting source for PL measurements.

3. Results and discussion

3.1. Effect of Zn/O flux ratio

Recent reports have demonstrated that the ZnO layers grown under the stoichiometric and/or the slight Zn-rich flux conditions showed better crystalline qualities due to the better surface migration of the adatoms [25,26]. Fig. 1 shows the growth rates of ZnO, which was grown directly on sapphire substrates without buffer layers, estimated from the cross-sectional SEM images as a function of reciprocal Zn temperature. On the whole, the flux of solid source is an exponential function of the reciprocal temperature in a suitable range. As shown in Fig. 1, the ZnO growth rate linearly increases up to near 310 °C and then saturates at higher Zn temperature. This behavior indicates that the growth mode is limited by the minority atom on the surface. When the growth rate is governed under oxygen-rich conditions, the growth rate linearly increases when Zn beam flux increases. When the Zn/O flux ratio is close to unity (i.e. the stoichiometric flux condition) the growth rate displays a gradual increase. Finally, the growth condition gets into Zn-rich, as the growth rate becomes saturated with further increases in Zn beam flux.

Fig. 2 shows the root-mean-square surface roughness of the ZnO films over the scanned size of 5 μm × 5 μm with different Zn temperature. The smallest roughness occurred at near the stoichiometric conditions due to the better surface migration of the adatoms [25,26].

Fig. 3 displays the 10 K normalized PL spectra measured at the near band edges from ZnO epilayers. The spectra show exciton emissions at 3.357, 3.361, and 3.376 eV. According to their energy, these emission lines can be ascribed to excitons bound to neutral donors ($D^{\circ}X$) and free excitons (FX_A), respectively. However, the spectra of samples, which were grown under near-stoichiometric growth conditions (Zn = 310 and 315 °C), revealed an energy red-shift of about 2 meV. This indicates that a small amount residual strain of ZnO epilayer was further relaxed under stoichiometric growth conditions due to the better surface migration of the adatoms. The (0 0 0 2) XRD measurements of ZnO epilayers, as shown in Fig. 4, agreed with the results of PL. The larger angle peaks in each spectrum are due to the Kα2 line of the X-ray source, and the diffraction angles of all spectra have been shifted to get the same angle from the sapphire substrates in different samples. Because of the compressive residual strain in ZnO epilayer, the lattice constant of *c*-axis became smaller as the strain was further relaxed under stoichiometric growth conditions.

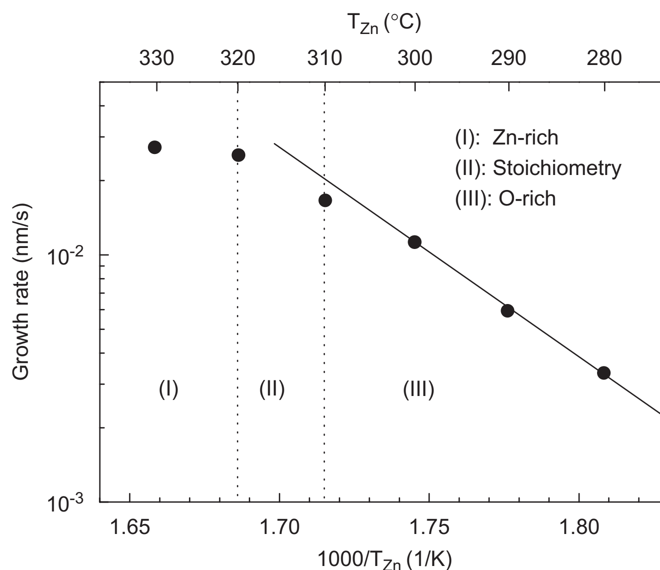

Fig. 1. Growth rates of ZnO films, grown under various Zn temperatures with fixed O-plasma conditions, estimated from the cross-sectional SEM images as a function of reciprocal Zn temperature. The solid line is the linear fitting of the lower-temperature region.

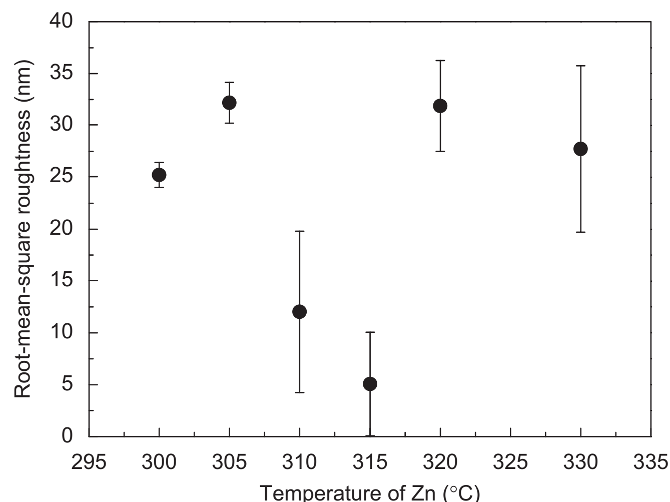

Fig. 2. Root-mean-square surface roughness of the ZnO films, grown under various Zn temperatures with fixed O-plasma conditions, over the scanned size of 5 μm × 5 μm as a function of Zn temperature.

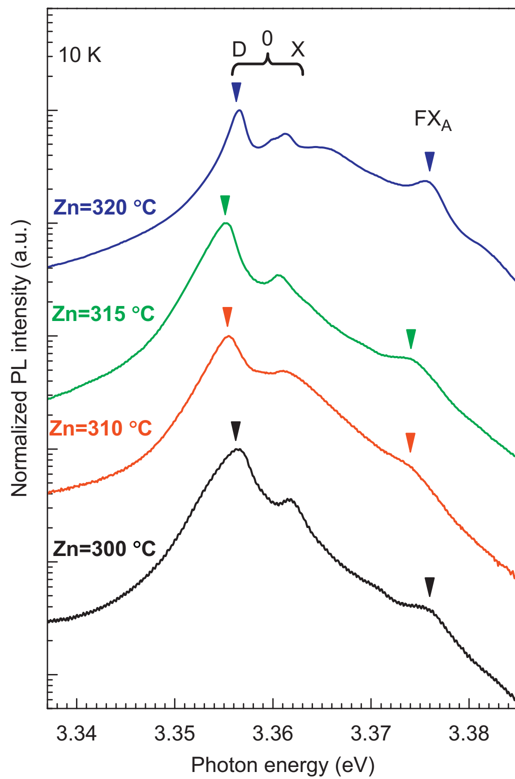

Fig. 3. Normalized 10 K PL spectra measured at the near band edge from ZnO epilayers grown under various Zn temperatures with fixed O-plasma conditions.

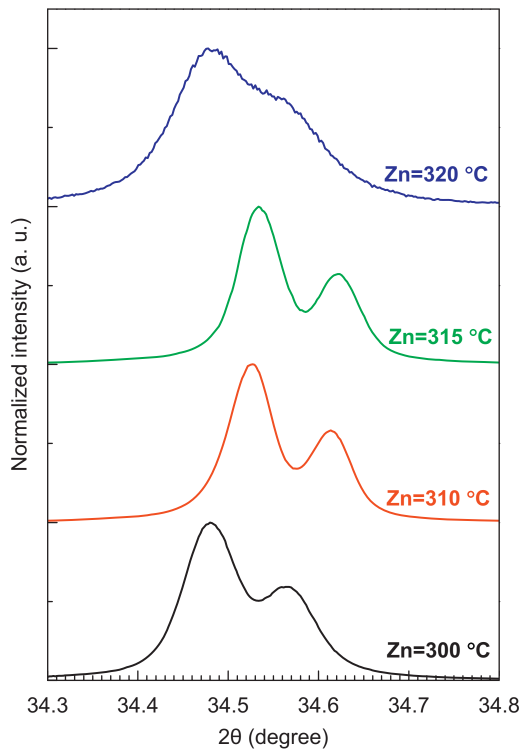

Fig. 4. Normalized (0 0 0 2) XRD spectra of ZnO epilayers grown under various Zn temperatures with fixed O-plasma conditions. The larger angle peaks in each spectrum are due to the Kα2 line of the X-ray source.

3.2. Effect of Mn-doped ZnO buffer

Fig. 5b and c shows the RHEED patterns of 6 nm-thick ZnO and Mn-doped ZnO (ZnO:Mn) at substrate temperature of 650 °C, respectively. The sapphire substrate displays a sharp streaky pattern, as shown in Fig. 5a, directly after oxygen plasma treatment, indicating a clean and flat surface. A 30° rotation in the basal plane of the ZnO layer was observed by RHEED, and the [1 $\bar{1}$ 0 0] direction of ZnO was found to align with the [1 1 $\bar{2}$ 0] direction of Al_2O_3. This indicates the ZnO lattice aligns itself with the oxygen sublattice in Al_2O_3, and the lattice mismatch is reduced from 32% to around 18% [13]. The RHEED patterns show that the crystal structure of ZnMnO buffer layers is the same as that of the ZnO. Besides, the in-plane lattice mismatch between the sapphire substrate and the 6 nm-thick ZnO and ZnO:Mn layers was estimated from the rod spacing of RHEED patterns to be around 12.1% and 15.4%, respectively. Moreover, AFM measurements revealed the root-mean-square surface roughness of the ZnO and ZnO:Mn layers was about 0.4 and 0.1 nm, respectively. We determined the concentration of Mn in this 6 nm-thick ZnO:Mn epilayer is less than 0.6% through the X-ray photoelectron spectroscopy (XPS) measurements. Our results suggest that a

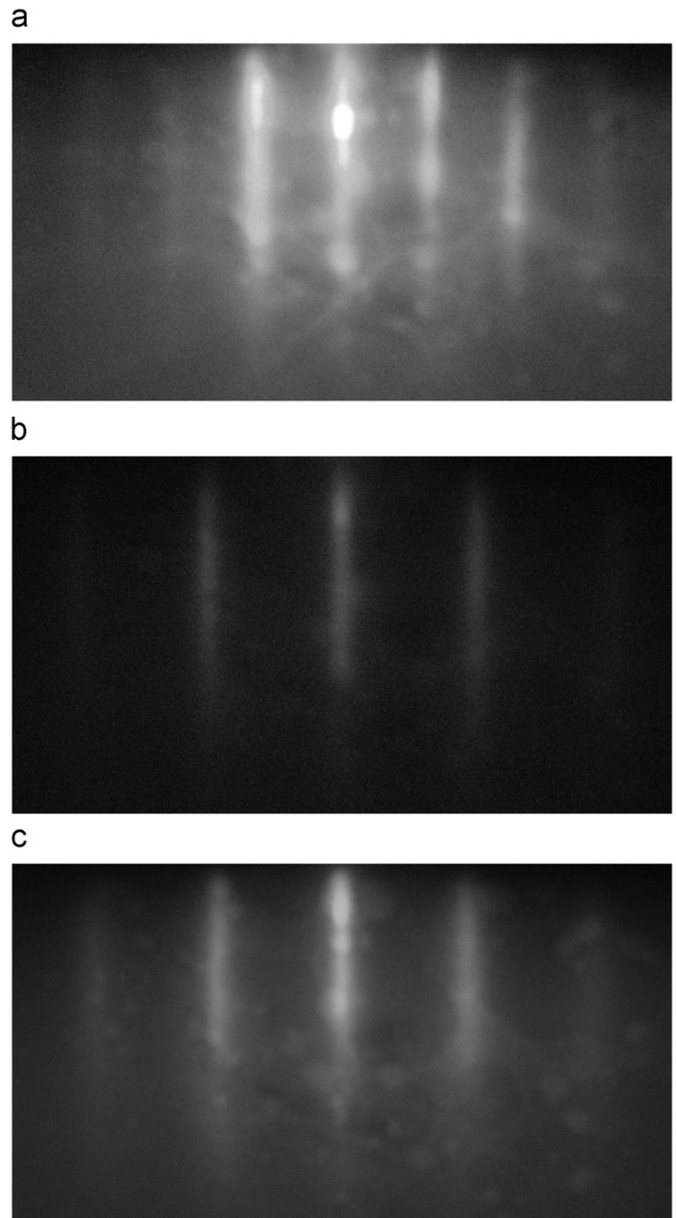

Fig. 5. RHEED patterns of (a) the sapphire substrate after oxygen plasma treatment, Al_2O_3 [1 1 $\bar{2}$ 0], (b) 6 nm-thick ZnO epilayer, ZnO [1 1 $\bar{2}$ 0], and (c) 6 nm-thick ZnO:Mn epilayer, ZnO:Mn [1 1 $\bar{2}$ 0]. The substrate temperatures were 650 °C.

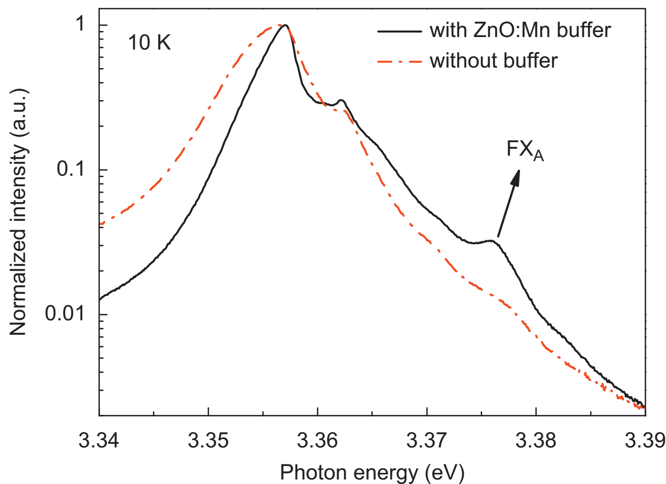

Fig. 6. Normalized 10 K PL spectra measured at the near band edge from 0.25 μm-thick ZnO epilayers grown under near stoichiometric growth conditions with and without 6 nm-thick ZnO:Mn buffer layers, respectively.

small amount of Mn doping greatly enhanced surface migration of the adatoms, and led to obtain a flatter surface with stronger lattice relaxation. Therefore, the ZnO:Mn layer could be a very promising buffer for the growth of high-quality ZnO.

Fig. 6 shows the 10 K normalized PL spectra measured at the near band edges from 0.25 μm-thick ZnO epilayers grown under near-stoichiometric growth conditions with and without 6 nm-thick ZnO:Mn buffer layers, respectively. By comparison the sample with ZnO:Mn buffer layer shows the much stronger FX_A emission and the smaller FWHM of D°X peak. On the other hand, decreased defect and/or dislocation density might result in a lower residual carrier concentration, and a higher mobility due to the decreased concentration of scattering centers. Hall measurements showed the mobility was enhanced from 24 to 50 $cm^2/V\,s$, and residual carrier concentration decreased from 1.4×10^{19} to $4.3\times10^{18}\,cm^{-3}$ by adding a 6 nm-thick ZnO:Mn buffer layer, indicating that this initial ZnO:Mn buffer layer could improve the crystalline quality of ZnO film.

4. Conclusion

The effects of the Zn/O flux ratio and the ZnO:Mn buffer layers on the material properties of ZnO epilayers grown by PA-MBE were investigated. A small amount of residual strain of ZnO epilayer was further relaxed under stoichiometric growth conditions, and caused a red-shift of near band edge emissions. Moreover, we proposed a ZnO:Mn buffer layer with simple growth process for the ZnO PA-MBE growth on *c*-plane sapphire substrates. A small amount of Mn doping could greatly enhance surface migration of the adatoms, and led to obtain a flatter surface with stronger lattice relaxation. Our results demonstrated that by using a ZnO:Mn buffer layer the optical and electrical properties of the ZnO epilayers had significant improvement.

Acknowledgments

This work was supported by the National Science Council of the Republic of China, Taiwan, under grant numbers NSC 95-2112-M-033-008-MY3. The authors are grateful for the support from the National Nano-Device Lab.

References

[1] D.M. Bagnall, Y.F. Chen, Z. Zhu, T. Yao, S. Koyama, M.Y. Shen, T. Goto, Appl. Phys. Lett. 70 (1997) 2230.
[2] Z.K. Tang, G.K.L. Wong, P. Yu, M. Kawasaki, A. Ohmoto, H. Koinuma, Y. Segawa, Appl. Phys. Lett. 72 (1998) 3270.
[3] D.M. Bagnall, Y.F. Chen, Z. Zhu, T. Yao, M.Y. Shen, T. Goto, Appl. Phys. Lett. 73 (1998) 1038.
[4] H. Ohno, Science 281 (1998) 951.
[5] S.J. Pearton, et al., J. Appl. Phys. 93 (2003) 1.
[6] T. Dietl, H. Ohno, F. Matsukura, J. Cibert, D. Ferrand, Science 287 (2000) 1019.
[7] T. Fukumura, Z. Jin, A. Ohtomo, H. Koinuma, M. Kawasaki, Appl. Phys. Lett. 75 (1999) 3366.
[8] T. Fukumura, Z. Jin, M. Kawasaki, T. Shono, T. Hasegawa, S. Koshihara, H. Koinuma, Appl. Phys. Lett. 78 (2001) 958.
[9] K. Sato, H. Katayama-Yoshida, Jpn. J. Appl. Phys. Part 2 40 (2001) L334.
[10] Y. Chen, D.M. Bagnall, Z. Zhu, T. Sekiuchi, K. Park, K. Hiraga, T. Yao, S. Koyama, M.Y. Shen, T. Goto, J. Crystal Growth 181 (1997) 165.
[11] P. Fons, K. Iwata, S. Niki, A. Yamada, K. Mastubara, M. Watanabe, J. Crystal Growth 201/202 (1999) 627.
[12] K. Sakurai, M. Kanehiro, K. Nakahara, T.T. Tanabe, Sz. Fujita, Sg. Fujita, J. Crystal Growth 214/215 (2000) 92.
[13] Y. Chen, D.M. Bagnall, H.J. Koh, K.T. Park, K. Hiraga, Z. Zhu, T. Yao, J. Appl. Phys. 84 (1998) 3912.
[14] H. Kato, M. Sano, K. Miyamoto, T. Yao, Jpn. J. Appl. Phys. Part 1 42 (2003) 2241.
[15] C. Liu, S.H. Chang, T.W. Noh, M. Abouzaid, P. Ruterana, H.H. Lee, D.W. Kim, J.S. Chung, Appl. Phys. Lett. 90 (2007) 011906.
[16] A.B.M. Almamun Ashrafi, N.T. Binh, B. Zhang, Y. Segawa, Appl. Phys. Lett. 84 (2004) 2814.
[17] H.C. Ong, A.X.E. Zhu, G.T. Du, Appl. Phys. Lett. 80 (2002) 941.
[18] K. Nakahara, H. Takasu, P. Fons, K. Iwata, A. Yamada, K. Matsubara, R. Hunger, S. Niki, J. Crystal Growth 227/228 (2001) 923.
[19] Y.S. Jung, O. Kononenko, J.S. Kim, W.K. Choi, J. Crystal Growth 274 (2005) 418.
[20] Y. Chen, H.J. Ko, S.K. Hong, T. Yao, Appl. Phys. Lett. 76 (2000) 559.
[21] K. Miyamoto, M. Sano, H. Kato, T. Yao, Jpn. J. Appl. Phys. 41 (2002) L1203.
[22] S.S. Kim, J.H. Moon, B.T. Lee, O.S. Song, J.H. Je, J. Appl. Phys. 95 (2004) 454.
[23] J. Han, P.Q. Mantas, A.M.R. Senos, J. Am. Ceram. Soc. 88 (2005) 1773.
[24] M. Nakayama, H. Tanaka, K. Masuko, T. Fukushima, A. Ashida, N. Fujimura, Appl. Phys. Lett. 88 (2006) 241908.
[25] H.J. Ko, T. Yao, Y. Chen, S.K. Hong, J. Appl. Phys. 92 (2002) 4354.
[26] A. Setiawan, Z. Vashaei, M.W. Cho, T. Yao, H. Kato, M. Sano, K. Miyamoto, I. Yonenaga, H.J. Ko, J. Appl. Phys. 96 (2004) 3763.